

shells which are considered to be homogeneous. It is also suitable for application to plates or shells when effects associated with transverse normal strain (or stress) are considered.<sup>8</sup> It is reported in Ref. 8 that sometimes this effect may exceed that of transverse shear.

### References

- <sup>1</sup> Ambartsumyan, S. A., *Theory of Anisotropic Shells*, NASA TT F-118, May 1964, Chap. II, p. 34.
- <sup>2</sup> Calcote, L. R., *The Analysis of Laminated Composite Structures*, Van Nostrand Reinhold, New York, 1969, Chap. 3, p. 53.
- <sup>3</sup> Lehnitskii, S. G., *Anisotropic Plates*, Gordon and Breach, New York, 1968, Chap. 9, p. 301.
- <sup>4</sup> Chou, P. C. et al., "Elastic Constants of Layered Media," *Journal of Composite Materials*, Vol. 6, 1972, p. 80.
- <sup>5</sup> Whitney, J. M., "The Effect of Transverse Shear Deformation on the Bending of Laminated Plates," *Journal of Composite Materials*, Vol. 3, 1969, p. 534.
- <sup>6</sup> Ashton, J. E. and Whitney, J. M., *Theory of Laminated Plates*, Technomic, Stamford, Conn., 1970.
- <sup>7</sup> Ambartsumyan, S. A., *Theory of Anisotropic Plates*, Technomic, Stamford, Conn., 1970.
- <sup>8</sup> Ambartsumyan, S. A., "A New Refined Theory of Anisotropic Shells," *Mechanika Polimerov*, No. 5, 1970, p. 884.

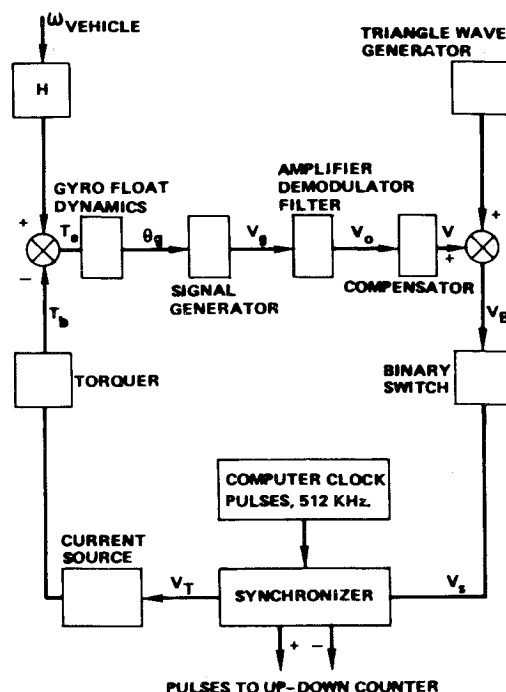


Fig. 1 Block diagram of complete system.

## Analysis and Test of a Precision Pulse-Rebalance Gyroscope

R. N. CLARK\*

University of Washington, Seattle, Wash.

AND

D. C. FOSTH†

The Boeing Company, Seattle, Wash.

### Introduction

THE advantages of pulse-rebalance schemes for inertial instruments, as compared to continuous rebalance techniques, are especially important where a digital computer is used to process the signals provided by these instruments.<sup>1-7</sup> A method for deriving the rebalance signal which uses a triangular wave modulation of the gyro signal is described here. This method is intended for use in strapdown attitude reference systems of advanced spacecraft and missiles.<sup>3</sup>

The purpose of the analysis and tests described here was twofold. First, a compensation network which assured a high static gain of the control loop and stability was required. Without this compensation the control loop exhibited a prominent limit cycle oscillation, which had to be eliminated by the compensation. Second, the steady-state accuracy of the entire system was to be determined to assess the suitability of this instrument

for strap-down applications. Both attitude and attitude rate can be determined from the signal provided by this instrument.

### Discrete Pulse-Width Modulated Rebalance System

The gyroscope used here is a Honeywell model GG334A3 single degree of freedom, gas bearing rotor, floated instrument. A block diagram of the entire gyro control loop showing how the digital signal is provided appears in Fig. 1. The transfer function representing the float dynamics is

$$\theta_g(s)/T_e(s) = (1/J)/s(s + C/J)$$

where  $C$  and  $J$  have the numerical values listed in Table 1. The signal generator is excited by 8 volts (rms) at a precisely controlled frequency of 6.4 KHz, giving the sensitivity listed in Table 1. A conventional phase-sensitive demodulator (with amplification) produces a full-wave rectified signal whose average value is proportional to  $\theta_g$ , the angular deflection of the output axis. The sensitivity of the amplifier-demodulator combination is 9 v (average value) per volt (rms). An active filter is used to smooth the full wave rectified output from the demodulator and to provide gain. The dynamics of this filter are chosen so that very little distortion of the (relatively) slowly fluctuating signal will occur while considerable smoothing of

Table 1 Physical characteristics of Honeywell GG334A3 gyroscope

Wheel momentum, $H$	$2 \times 10^5 \text{ GR}(\text{cm})^2(\text{sec})^{-1}$
Moment of inertia of float Assembly about output axis, $J$	$225 \text{ GR}(\text{cm})^2$
Damping coefficient of Float about output axis, $C$	$2.5 \times 10^5 \text{ dyne-cm-sec.}$
Signal generator sensitivity, (Excitation 8 v, 6.4 KHz)	18.7 mv (rms) per mrad
Torquer sensitivity	$1.03 \times 10^3 \text{ dyne-cm per ma}$

Received June 18, 1973; revision received November 2, 1973. The authors wish to acknowledge the contributions to the electronic design of the digital circuits and the design of the demodulator filters made by J. M. Folline and R. VanSickle. Constructive suggestions by the reviewers are also acknowledged.

Index categories: Data Sensing and Presentation or Transmission Systems; Spacecraft Attitude Dynamics and Control.

\* Professor of Electrical Engineering; also Consultant, The Boeing Company, Sensors, Guidance, and Control Dept., Aerospace Group.

† Senior Specialist Engineer, Sensors, Guidance, and Control Dept., Aerospace Group.

the sharp peaked carrier will be realized. The transfer function of this filter is

$$32 \left[ \frac{\omega_n^2}{s^2 + 2\zeta\omega_n s + \omega_n^2} \right]^2$$

where  $\zeta = 0.7$  and  $\omega_n = 3.8 \times 10^4$  rad/sec. For purposes of control loop dynamic analysis this filter can be represented as a simple gain of 32. However, the attenuation of this filter at 6.4 KHz and 12.8 KHz is important for the suppression of the limit-cycle oscillation of the system. Following the filter is a compensating amplifier which provides further attenuation of the 6.4 KHz and 12.8 KHz ripple and conventional lag-lead compensation. The transfer function for this compensator is

$$V(s)/V_0(s) = 132 \times 10^6 (s + 500) / (s + 20)(s + 5000)^2$$

The static gain of the forward loop is therefore  $V/\theta_g = 710$  v/mrad.

The output of the compensator is summed with a 1000 Hz triangular voltage of amplitude  $h$ , and the sum actuates a binary switch, as indicated in Figs. 1 and 2. The binary output is synchronized with the 512 KHz computer clock pulses. Therefore  $V_T(t)$  is a rectangular wave having a repetition rate of 1 KHz and zero crossings which occur only at discrete instants coincident with the computer clock pulses. Further,  $V_T(t)$  is pulse-width modulated by an amount proportional to (in a quantized fashion)  $V(t)$ . Figure 2 illustrates the situation for a constant  $V(t)$ .  $V_T(t)$  switches a precise current source so that the current pulses into the torquer have the same waveform (ideally) as  $V_T(t)$ . There is an  $L/R$  time lag in the torquer circuit, but this does not change the average value of the current in the torquer from the average value of the ideal current shown in Fig. 2. It introduces a dynamic lag in the loop which may be accounted for by conventional means. The current source used in this system is 28.8 ma, sufficient to rebalance an inertial torque corresponding to a vehicle rate of 8.5 deg/sec. If  $V(t)$  is constant the two pulse widths  $\tau^+$  and  $\tau^-$  shown in Fig. 2 will also be constant so that the average value of torquer current will be

$$i_{AV} = (28.8)[(\tau^+ - \tau^-)/0.001] \text{ ma}$$

100% modulation occurs for  $V(t) = h$ , so for purposes of linear analysis the static gain of the feedback path is

$$i_{AV}/V = 28.8/h \text{ ma/v}$$

An  $h$  of 8 volts was employed. The salient characteristics of the electronic portion of the system are listed in Table 2.

The up-down counter receives 512,000 pulses per sec, the sign of each pulse is the sign of  $V_T$  immediately following each computer clock instant. If, for example,  $V(t)$  is zero the counter will receive a train of 256 positive pulses followed by a train of 256 negative pulses during each msec period. When  $V(t)$  is nonzero there will be a net difference in the number of positive and the number of negative pulses—that difference will correspond in sign to the sign of  $V(t)$  and in magnitude to the (quantized) magnitude of  $V(t)$ . The counter provides the on-board digital computer with the basic data from which vehicle attitude and attitude rate are determined. Because the maximum vehicle rate which can be accommodated in this system is about 8.5 deg/sec and the pulse count rate is 512,000 per sec, the resolution of the vehicle attitude measurement could not be finer than 0.06 second of arc.

Previously sawtooth waveforms have been used in pulse rebalance systems where the triangle waveform is used in this

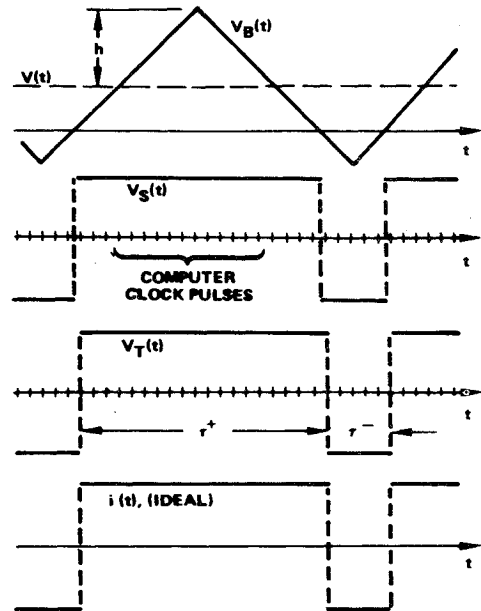


Fig. 2 Illustrating the discrete pulse-width modulation of  $V_T(t)$ .

one.<sup>1,2</sup> The triangle waveform has some advantages over the sawtooth, especially where the computer clock rate is high. Electronic switching in the triangle wave circuitry occurs at the instant  $V_B(t)$  reaches its maximum value, virtually outside the modulation range, whereas it occurs at a zero crossing in the sawtooth circuitry. For a computer clock rate in the megahertz range, which appears feasible, this is an advantage in accuracy of pulse count. Because there are two zero crossings of  $V_B(t)$  per cycle, one ascending and one descending, in the triangle wave, as compared to only one, unidirectional, with the sawtooth wave, less error in pulse count is realized for small errors in the zero crossing instants.

With the numerical values indicated above, and in Tables 1 and 2, the loop transfer function, for linear stability analysis is

$$\frac{T_b(s)}{T_e(s)} = \frac{8.4 \times 10^{16}(s + 500)}{s(s + 1110)(s + 20)(s + 5000)^2(s + 7150)}$$

The gain margin is therefore approximately 1.9 and the steady-state float offset is only about 0.25 sec of arc per degree per second of vehicle rate.

There is a steady oscillation of the gyro float at 1000 Hz due to the modulation of the torquer current at this frequency. The magnitude of this oscillation will be less than 1.7 arc sec (peak to peak) when the vehicle rate is zero, and even smaller for nonzero rates. This oscillation is not large enough to cause  $V_T(t)$  to cross zero at a clock pulse different from the one it would cross at if the oscillation were absent.

#### Experimental Results

The gyro was mounted on a Fecker precision rate table, which is capable of rates up to 200 earth rate units (0.833 deg/sec) with an accuracy of  $\pm 4.2 \times 10^{-6}$  deg/sec, exclusive of the periodic inaccuracies of wow and flutter. Tests were run at 25, 50, 100, and 200 earth rate units. The up-down counter sums the positive and negative pulses for a preset time period of approximately 100 sec, which is accurately known from a precision time base. The sum represents the total vehicle angle change during the summation period, and, if divided by the known period, yields vehicle rate. It was necessary to average the results obtained over several 100 second runs (at each table rate) due to the wow and flutter of the table. Accuracy measurements using this technique were found to be repeatable and showed that the linearity of the instrument was 0.01% of the maximum

Table 2 Physical characteristics of pulse rebalance electronics

Signal generator excitation frequency	6.4 KHz
Triangle generator frequency	1.0 KHz
Triangle generator voltage $h$	8 v
Computer clock frequency	512 KHz
Time constant of torquer circuit	140 $\mu$ sec

rate used, which is only one tenth of the full scale capability of this instrument.

To test the system over its full dynamic range another series of steady-state tests was run using a precision current source (North Hills) applied to a second torquer which happens to exist on the output axis of the gyro. Current corresponding to vehicle rates up to 8 deg/sec was applied and the same averaging techniques described above were used to eliminate the influence of current noise. Again, the linearity proved to be 0.01% of the maximum rate.

Transient response tests were run on this system to assess the control loop stability.

These tests confirmed that the linear analysis was useful in determining large-signal stability. It was also shown that a limit cycle oscillation of approximately 100 Hz will exist if the 6.4 KHz ripple present in  $V(t)$  is too large. The amplitude of this oscillation increases as the ripple amplitude increases and it can be observed as a fluttering of the edge of the pulse train at the output of the synchronizer. The filter and compensator described above eliminated this limit cycle oscillation. However, a slight flutter, one clock pulse width in magnitude, exists even when  $V(t)$  is reduced to zero. This appears to be inherent in the binary switch and not dependent on the other parameters in the system.

#### References

- <sup>1</sup> Scoville, A. E. and Yamron, J., "The Mechanization of a Strapdown Inertial System Based on Time-Modulated Torquing," AIAA/JACC Guidance and Control Conf., Seattle, Wash., Aug. 1966, pp. 136-148.
- <sup>2</sup> Roantree, J. P. and Kormanik, N. J., "A Generalized Design Criterion for Strapped-Down Inertial Sensor Loops," AIAA/JACC Guidance and Control Conf., Seattle, Wash., Aug. 1966, pp. 149-162.
- <sup>3</sup> Fehr, T. D., Fosth, D. C., and McDonald, R. K., "High Accuracy Approach Guidance System for Grand Tour," AIAA Paper 72-867, Stanford, Calif., 1972.
- <sup>4</sup> Otten, D. D., "A Look into Strapdown Guidance—I," *Control Engineering*, Oct. 1966, pp. 61-67.
- <sup>5</sup> Lory, C. B., "Compensation of Pulse-Rebalanced Inertial Instruments," Rept. T-495, Jan. 1968, MIT/IL, Cambridge, Mass.
- <sup>6</sup> Gilmore, J. P. and Feldman, J., "Gyroscope in Torque-to-Balance Strapdown Application," *Journal of Spacecraft and Rockets*, Vol. 7, No. 9, Sept. 1970, pp. 1075-1082.
- <sup>7</sup> Gilmore, J. P. and McKern, R. A., "Strapdown Inertial Attitude-Indication Evaluations," *Journal of Spacecraft and Rockets*, Vol. 7, No. 7, July 1970, pp. 825-831.

## Mission Planning Aspects of Skylab Earth Resources Experiments

DAVID D. DEATKINE\*

NASA Johnson Space Center, Houston, Texas

#### Introduction

ONE of the major objectives of the Skylab program is the return and processing of Earth resources data taken with a set of multispectral remote sensors, referred to collectively as

the Earth Resources Experiments Package (EREP). The Skylab orbital workshop (OWS) was launched in late spring of 1973 to circle the Earth in a controlled 234-naut mile altitude circular orbit. The workshop was visited by a crew of three, aboard an Apollo command and service module (CSM), on three occasions during the 8-month lifetime of the orbiting laboratory. This schedule allowed observation of the Earth under a variety of seasonal conditions.

#### Mission Requirements

The EREP mission requirements consist of a comprehensive set of objectives aimed at obtaining data for both sensor performance evaluation and Earth resources applications. The pre-determined, calibrated sites, nearly 700 in number, are distributed world-wide, but are concentrated mostly in the U.S. and surrounding coastal areas. Other targets, such as hurricanes and active volcanoes, are to be determined in real-time. Earth resources experiments were submitted by more than 130 American and foreign principal investigators and range from regional planning and agriculture to oceanography and weather observation. Each experiment specifies for its associated sites a detailed set of required conditions for data taking. These conditions include such parameters as sun angle, season, number of data takes, acceptable cloud cover, and instrument requirements. The task of completing a maximum number of these proposals through mission planning is complicated by the wide variety of required site conditions encountered on any given EREP pass.

#### EREP Pass Planning Considerations and Methods

The EREP data passes are performed in a local-vertical (Z-LV) attitude hold.<sup>†</sup> Because this attitude is a deviation from the normal solar inertial (SI)<sup>‡</sup> mode for thermal and power design reasons, these Z-LV holds must be constrained in duration, number, and solar angular relationship. The Z-LV constraints are briefly as follows: a) the angle between the sun-Earth line and the orbit plane (known as the beta angle) must be within  $\pm 65^\circ$ ; b) the Z-LV pass length should be less than  $160^\circ$  orbital angle; and c) there should be no more than three Z-LV passes per day.

The total number of Z-LV EREP passes originally available for all three Skylab missions was 60; however, this constraint was removed, and for the later two missions the number is dependent on available consumables. Other constraints which significantly affect EREP operations are terrain lighting conditions and weather (cloud cover); weather conditions over EREP sites greatly affect data takes and are discussed later with the real-time operations. In the premission planning, clear weather is assumed.

#### Lighting Effects of Launch Time and Season

Almost all of the Earth resources proposals specify desired sun lighting conditions; most of these are daylight conditions with sun angles (measured with respect to the local horizontal) above  $20^\circ$ - $30^\circ$ . It is desirable, therefore, to design the launch time and date, if possible, to allow for maximum sun elevation angles in the northern hemisphere; the lighting is to be maximized in the U.S., where almost 80% of the EREP sites are defined. However, other mission factors are affected by launch time and date as well, some more constraining and considered more important than the EREP requirements. Shown in Fig. 1 is the effect of SL-1 (the OWS) launch data on subsequent adequately-lighted U.S. pass opportunities. A three-mission maximum

Presented as Paper 73-619 at the AIAA/ASME/SAE Joint Space Mission Planning and Execution Meeting, Denver, Colo., July 10-12, 1973; submitted August 27, 1973; revision received December 10, 1973.

Index categories: Earth-Orbital Trajectories; Space Station Systems, Manned.

\* Aerospace Engineer, Orbital Design Section, Mission Integration Branch, Mission Planning and Analysis Division.

<sup>†</sup> Some EREP data takes are planned while the orbital assembly (OA) is in the solar inertial mode (approximately five passes) under specific conditions; however, the discussion herein is restricted to the normal Z-LV attitude cases.

<sup>‡</sup> The solar inertial mode is an inertial attitude hold which points the OWS+Z axis at the sun.